Detecting Event Horizons and Stationary Surfaces

Richard G. Gass, F. Paul Esposito, L.C.R. Wijewardhana and Louis Witten

Department of Physics, University of Cincinnati, Cincinnati, OH 45220-0011

Abstract

We have investigated the behavior of three curvature invariants for Schwarzschild, Reissner-Nordstrøm, Kerr, and Kerr-Newman black holes. We have also studied these invariants for a Schwarzschild-de Sitter space-time, the γ metric, and for a 2+1 charged dimensional black hole. The invariants are $I_1 = R_{\alpha\beta\mu\nu;\lambda}R^{\alpha\beta\mu\nu;\lambda}$, $I_2 = R_{\mu\nu;\lambda}R^{\mu\nu;\lambda}$, and $I_3 = C_{\alpha\beta\mu\nu;\lambda}C^{\alpha\beta\mu\nu;\lambda}$. For all but the Kerr-Newman case these invariants serve as either horizon or stationary surface detectors. The Kerr-Newman case is more complicated. We show that I_1 vanishs on the horizon in any space-time with a Schwarzschild like metric.

I. INTRODUCTION

An outstanding challenge in the calculation of gravitational collapse to black hole configurations is the identification of emerging black holes in the data on space-like slices of the space time [1–3]. Since the definition of event horizons involves knowledge of the future evolution of the data, the computational situation is not as clear-cut as one would like. In fact, the computational burden is shifted towards the identification of apparent horizons, as discussed in the previously cited references. Hoping to alleviate some of this burden, we have tried to develop criteria, involving the curvature tensor and its derivatives, which would indicate the existence of black holes. These criteria would, ideally, be complementary to those involving marginally outer-trapped surfaces. These criteria also would indicate a

trend in the data towards the formation of black holes. This hope has been fulfilled only partially. We take the opportunity to correct a result which has previously appeared in the literature.

It has long been believed that an observer falling toward a black hole cannot tell when he or she has crossed the event horizon. This belief is based on the fact that the horizon is a global property of the geometry. The invariant

$$I_1 = R_{\alpha\beta\mu\nu;\lambda} R^{\alpha\beta\mu\nu;\lambda} \tag{1.1}$$

involves a covariant derivative of the curvature tensor and thus may be used to probe a neighborhood of the event horizon. This means that it has a chance of functioning as a horizon detector. This fact was first noticed by Karlhede, Lindström, and Åman [4] who calculated I_1 for the Schwarzschild, Reissner-Nordstrøm, Taub-NUT, and Kerr solutions. Karlhede, Lindström and Åman found that I_1 vanished on the event horizon for the Schwarzschild, Reissner-Nordstrøm, and Taub-NUT solutions, and that it vanished on the stationary surface for the Kerr solution. Our results differ from those of Karlhede *at el* by a sign and due to our sign convention which is that of Misner, Thorne, and Wheeler [5]. I_1 has also been investigated by Tammelo and Kask [6]. To our knowledge, the invariants

$$I_2 = R_{\mu\nu;\lambda} R^{\mu\nu;\lambda} \tag{1.2}$$

and

$$I_3 = C_{\alpha\beta\mu\nu;\lambda} C^{\alpha\beta\mu\nu;\lambda} \tag{1.3}$$

have not been previously investigated. The curvature invariants are, in principle, locally measurable quantities [4,6,7], and thus could allow the local detection of an event horizon or a stationary surface.

Using *Mathematica* and MathTensor, we have calculated I_1, I_2, and I_3 for the Kerr-Newman geometry and for the special cases of Kerr, Reissner-Nordstrøm, and Schwarzschild black holes. We have also computed I_1 for a Schwarzschild-de Sitter space-time, for the γ

metric [8], and for a charged 2+1 black hole space-time. On a 300 MegHz PowerMac G3 the calculations take several hours of run time for the longest (Kerr-Newman) cases. For vacuum space-times, $I_1 = I_3$ and, of course, $I_2 = 0$. We conjecture that I_1 serves as an event horizon detector for any static space-time where the horizon is regular. If the horizon is singular, it is not clear how to distingish the horizon from any other type of singularity.

In addition to being intrinsically interesting horizon detection is of considerable interest in numerical relativity. The ablility to track the causal structure of a space-time is believed to be a crucial step in numerically evolving black hole space-times [1]. For this reason considerable effort has gone into constructing apparent horizon finders in numerical relativity [2,3]. The invariants discussed here maybe useful in that regard.

II. STATIC AND STATIONARY SPACE-TIMES

We have investigated the behaviour of I_1 for both four dimensional space-times and a 2+1 black hole space-time.

A. Four Dimensional Space-Times

1. Schwarzschild black holes

We begin by discussing the Schwarzschild solution since it is the simplest case. For the Schwarzschild solution, the metric is

$$ds^2 = -(1 - 2M/r)dt^2 + (1 - 2M/r)^{-1}dr^2 + r^2(d\theta^2 + \sin^2\theta d\phi^2), \tag{2.1}$$

and we find that [4]

$$I_1 = -\frac{720\, M^2\, (2\, M - r)}{r^9}. \tag{2.2}$$

It is clear from equation (2.2) that the invariant is positive outside the event horizon, goes to zero on the event horizon, and is negative inside the event horizon. The invariant

has a maximum at $r = 9M/4$, and the only zeros of the invariant are at infinity and on the event horizon. An in-falling observer can thus detect the presence of the event horizon by monitoring I_1. The in-falling observer may, for instance, measure the variation in oscillation frequencies from the equation of geodesic deviation [6]. An in-falling observer can not save him or her self by turning back when the invariant vanishes for by that time it is too late! However, the invariant does provide a warning and the observer could turn back when the maximum of the invariant is reached.

2. Reissner-Nordstrøm black holes

The metric for the Reissner-Nordstrøm solution is

$$ds^2 = -(1 - 2M/r + Q^2/r^2)dt^2 + (1 - 2M/r + Q^2/r^2)^{-1}dr^2 + r^2(d\theta^2 + \sin^2\theta d\phi^2). \quad (2.3)$$

The Reissner-Nordstrøm case is somewhat more complicated, but the results for I_1 are essentially the same as those for the Schwarzschild solution: I_1 vanishes only at $r = \infty$, on the horizon r_+, and on the null surface r_-. There is a positive extremal value of I_1 just outside of r_+. The full invariant is

$$I_1 = \frac{16\left(76\,Q^4 - 108\,M\,Q^2\,r + 45\,M^2\,r^2\right)\left(Q^2 + r\,(-2\,M + r)\right)}{r^{12}}, \quad (2.4)$$

and we see that $I_1 = 0$ at $r = \infty$. The vanishing of I_1 can be reduced to finding the roots where the numerator of equation 2.4 vanishes.

There are two finite complex roots and two finite real roots. The two real roots are the null surface $r_- = M - \sqrt{M^2 - Q^2}$ and the event horizon $r_+ = M + \sqrt{M^2 - Q^2}$. This result was first obtained by Karlhede, Lindström and Åman [4], although there is a typographical error in their result for I_1 for the Reissner-Nordstrøm case. Figure one shows a typical plot of I_1 as a function of r in the vicinity of r_+ and figure two shows a typical plot of I_1 as a function of r in the vicinity of r_-. We notice that I_1 is positive outside r_+, negative in the region between r_+, and r_- and positive inside r_-. The complex roots occur at $r = \frac{2\left(9\,Q^2 - i\sqrt{14}\,Q^2\right)}{15\,M}$ and $r = \frac{2\left(9\,Q^2 + i\sqrt{14}\,Q^2\right)}{15\,M}$.

4

For the Reissner-Nordstrøm case, I_2

$$I_2 = \frac{80\, Q^4 \, (Q^2 + r\,(-2\,M + r))}{r^{12}}. \tag{2.5}$$

We observe that, like I_1, I_2 vanishes at r_+ and r_-, but that unlike I_1, I_2 has no complex roots. Figure three shows I_2 in the region of the horizon.

The invariant I_3 is given by

$$I_3 = \frac{48\,(Q^2 - 2\,M\,r + r^2)\,(22\,Q^4 - 36\,M\,Q^2\,r + 15\,M^2\,r^2)}{r^{12}}. \tag{2.6}$$

Like I_1 and I_2, I_3 vanishes at r_+ and r_-. In addition I_3 has two complex roots which lie at $r = \frac{18\,Q^2 - i\,\sqrt{6}\,Q^2}{15\,M}$ and $r = \frac{18\,Q^2 + i\,\sqrt{6}\,Q^2}{15\,M}$. The complex roots of I_1 and I_3 are not the same but near the horizon I_1 and I_3 are numerically close in the sense that $|(I_1 - I_3)/I_1| \ll 1$. Figure four shows the difference between I_1 and I_3 in the vicinity of the horizon for a particular choice of parameters.

For an extremal black hole $Q = M$ the two roots at r_+ and r_- coalesce into a double root at $r = M$. If $Q^2 > M^2$, then I_1, I_2, and I_3 have no real roots.

3. Schwarzschild-de Sitter spacetimes

For the Schwarzschild-de Sitter space-time the metric is

$$ds^2 = -(1 - 2M/r + \Lambda r^2/3)dt^2 + (1 - 2M/r + \Lambda r^2/3)^{-1}dr^2 + r^2(d\theta^2 + \sin^2\theta d\phi^2), \quad (2.7)$$

and

$$I_1 = \frac{240\, M^2\,(-6\,M + 3\,r - r^3\,\Lambda)}{r^9}. \tag{2.8}$$

This invariant is zero when $1 - 2M/r - \Lambda r^2/3 = 0$, which is the event horizon. Thus, I_1 seems to serve as a cosmological event horizon detector.

We call a Schwarzschild like metric one with the line element

$$ds^2 = -A(r)dt^2 + A(r)^{-1}dr^2 + r^2 d\theta^2 + r^2 \sin^2\theta d\phi^2. \tag{2.9}$$

where $A(r)$ is an arbitrary function of r. For this metric we can calculate I_1 for a general $A(r)$ and we find that

$$I_1 = A(r) \left[\left(32 + 32\, A(r)^2 + 16\, r^2\, A'(r)^2 - 32\, A(r)\, (2 + r\, A'(r)) \right. \right.$$
$$\left. \left. + 8\, r^4\, A''(r)^2 - 16\, r\, A'(r)\, \left(-2 + r^2\, A''(r) \right) + r^6\, A'''(r)^2 \right) \right] / r^6, \tag{2.10}$$

where the primes indicate differentiation with respect to r. We notice that I_1 vanishes when $A(r)$, the norm of the time-like Killing vector, vanishes. In addition I_1 will vanish when

$$32 + 32\, A(r)^2 + 16\, r^2\, A'(r)^2 - 32\, A(r)\, (2 + r\, A'(r))$$
$$+ 8\, r^4\, A''(r)^2 - 16\, r\, A'(r)\, \left(-2 + r^2\, A''(r) \right) + r^6\, A'''(r)^2 = 0. \tag{2.11}$$

With the appropriate choices for $A(r)$, I_1 reduces to either the Schwarzschild or the Reissner-Nordstrøm result. We have also calculated the invariants I_2 and I_3 for this space-time and find that

$$I_2 = A(r) \left[\left(24 + 24\, A(r)^2 + 4\, r^2\, A'(r)^2 + 24\, r^2\, A''(r) + 10\, r^4\, A''(r)^2 - \right. \right.$$
$$24\, A(r)\, \left(2 + r^2\, A''(r) \right) + 4\, r^5\, A''(r)\, A^{(3)}(r) + r^6\, A'''(r)^2 -$$
$$\left. \left. 4\, r^3\, A'(r)\, \left(2\, A''(r) + r\, A'''(r) \right) \right) \right] / 2\, r^6 \tag{2.12}$$

and

$$I_3 = A(r) \left[\left(40 + 40\, A(r)^2 + 40\, r^2\, A'(r)^2 - 40\, r^2\, A''(r) + 10\, r^4\, A''(r)^2 + 8\, r^3\, A'''(r) - 4\, r^5\, A''(r)\, A'''(r) + \right. \right.$$
$$r^6\, A'''(r)^2 + 8\, r\, A'(r)\, \left(10 - 5\, r^2\, A''(r) + r^3\, A'''(r) \right) - 8\, A(r)\, (10 + 10\, r\, A'(r) -$$
$$\left. \left. 5\, r^2\, A''(r) + r^3\, A'''(r) \right) \right] / 3\, r^6. \tag{2.13}$$

If the space-time is a vacuum space-time then the field equations imply

6

$$A'(r) = \frac{1 - A(r)}{r} \tag{2.14}$$

and $I_2 = 0$, while

$$I_1 = I_3 = \frac{180\,(-1 + A(r))^2\,A(r)}{r^6}. \tag{2.15}$$

5. Kerr Black Holes

The metric for the Kerr solution is

$$ds^2 = \rho^2\left(\frac{dr^2}{\Delta} + d\theta^2\right) + (r^2 + a^2)\sin^2\theta d\phi^2 - dt^2 + \frac{2Mr}{\rho^2}\left(a\sin^2\theta d\phi - dt\right)^2, \tag{2.16}$$

where $\rho^2(r,\theta) = r^2 + a^2\cos^2\theta$ and $\Delta(r) = r^2 - 2Mr + a^2$. For Kerr black holes the only invariant of interest is I_1, and we find the remarkably simple result that

$$\begin{aligned}
I_1 = {}& 368640\,M^2\left(-2\,M\,r + r^2 + a^2\cos(\theta)^2\right) \times \\
& \frac{\left(r^8 - 28\,a^2\,r^6\cos(\theta)^2 + 70\,a^4\,r^4\cos(\theta)^4 - 28\,a^6\,r^2\cos(\theta)^6 + a^8\cos(\theta)^8\right)}{\left(a^2 + 2\,r^2 + a^2\,\cos(2\,\theta)\right)^9}.
\end{aligned} \tag{2.17}$$

The form of our result is different from the one given by Karlhede *at el* [4] but the two agree up to the previously mentioned sign convention.

For the Kerr solution, the invariant I_1 has 10 roots. Two of these involve the mass of the hole and are at the inner and outer stationary limits given by $r_\pm = M \pm \sqrt{M^2 - a^2\cos^2\theta}$. The other eight roots depend only on a. The fact that I_1 vanishes at the stationary limit rather than the horizon is not surprising since the norm of the Killing vector $\frac{\partial}{\partial t}$ vanishes on the stationary surface. The Killing vector $\frac{\partial}{\partial t} + \Omega_H \frac{\partial}{\partial \phi}$,where $\Omega_H = \frac{a}{r_+^2 + a^2}$ is tangent to the null geodesic generators of the horizon. [9].

The eight Kerr roots that depend only on a may be expressed in a simple form and are given in Table 1. We observe that the roots are paired; for every root at a positive value of r there is a root at the corresponding negative value of r. Each root in the left column of Table 1 is paired with the corresponding root in the right column. The existence of roots for

negative values of r is perhaps not surprising since the maximally extended Kerr solution includes both positive and negative values of r [10]. As $a \to 0$, the mass independent roots coalesce to zero. If $a^2 > M^2$ then the two mass dependent roots become complex.

The zeros of I_1 are shown in figure 5. The behavior of I_1 in the vicinity of the horizon is shown in figure 6.

6. Kerr-Newman Black Holes

The most complicated case we consider is the Kerr-Newman black hole. The metric for the Kerr-Newman solution is

$$ds^2 = -(\Delta/\rho^2)\left(dt - a\sin^2\theta d\phi\right)^2 + (\sin^2\theta/\rho^2)\left[\left(r^2 + a^2\right)d\phi - adt\right]^2$$
$$+(\rho^2/\Delta)dr^2 + \rho^2 d\theta^2, \tag{2.18}$$

where $\rho^2(r,\theta) = r^2 + a^2\cos^2\theta$ and $\Delta(r) = r^2 - 2Mr + a^2 + Q^2$.

For the Kerr-Newman solution, all three invariants are distinct and in general do not vanish on either the horizon or on the stationary surface. We find that

$$
\begin{aligned}
I_1 = &\left[8192\left(r^6\left(76\,Q^6 - 260\,M\,Q^4\,r + 261\,M^2\,Q^2\,r^2 + 76\,Q^4\,r^2 - 90\,M^3\,r^3\right.\right.\right. \\
&\left.\left.-108\,M\,Q^2\,r^3 + 45\,M^2\,r^4 + a^2\left(44\,Q^4 - 36\,M\,Q^2\,r\right)\right) + a^2\,r^4\;\times \right. \\
&\left(-744\,Q^6 + 3540\,M\,Q^4\,r - 5364\,M^2\,Q^2\,r^2 - 712\,Q^4\,r^2 + 2520\,M^3\,r^3 + 1980\,M\,Q^2\,r^3- \right. \\
&\left.1215\,M^2\,r^4 + a^2\left(-156\,Q^4 + 324\,M\,Q^2\,r\right)\right)\cos(\theta)^2 + 6\,a^4\,r^2\left(98\,Q^6 - 706\,M\,Q^4\,r + 1545\,M^2\,Q^2\,r^2\right. \\
&\left.-1050\,M^3\,r^3 - 222\,M\,Q^2\,r^3 + 315\,M^2\,r^4 + a^2\left(-26\,Q^4 + 30\,M\,Q^2\,r\right)\right)\cos(\theta)^4+ \\
&2\,a^6\left(-16\,Q^6 + 302\,M\,Q^4\,r - 1170\,M^2\,Q^2\,r^2 + 356\,Q^4\,r^2 + 1260\,M^3\,r^3 - 1350\,M\,Q^2\,r^3 + 945\,M^2\,r^4+ \right. \\
&\left.2\,a^2\left(11\,Q^4 - 45\,M\,Q^2\,r\right)\right)\cos(\theta)^6 - a^8\left(76\,Q^4 + 90\,M^3\,r - 720\,M\,Q^2\,r - 45\,M^2\left(Q^2 - 27\,r^2\right)\right)\cos(\theta)^8+ \\
&\left.45\,a^{10}\,M^2\cos(\theta)^{10}\right)\right]/\left(a^2 + 2\,r^2 + a^2\cos(2\,\theta)\right)^9, \tag{2.19}
\end{aligned}
$$

$$
I_2 = \frac{-2048\,Q^4\left(-\left(r^2\left(4\,a^2 + 5\left(Q^2 - 2\,M\,r + r^2\right)\right)\right) - a^2\left(4\,a^2 - Q^2 + 2\,M\,r\right)\cos(\theta)^2 + 5\,a^4\cos(\theta)^4\right)}{\left(a^2 + 2\,r^2 + a^2\cos(2\,\theta)\right)^7}, \tag{2.20}
$$

and

$$
\begin{aligned}
I_3 = \Big[& 24576 \left(r^6 \left(22\,Q^6 - 80\,M\,Q^4\,r + 87\,M^2\,Q^2\,r^2 + 22\,Q^4\,r^2 - 30\,M^3\,r^3 - 36\,M\,Q^2\,r^3 + 15\,M^2\,r^4 + \right. \right. \\
& \left. 12\,a^2 \left(Q^4 - M\,Q^2\,r \right) \right) + a^2\,r^4 \left(-254\,Q^6 + 1192\,M\,Q^4\,r - 1788\,M^2\,Q^2\,r^2 - 244\,Q^4\,r^2 + \right. \\
& \left. 840\,M^3\,r^3 + 660\,M\,Q^2\,r^3 - 405\,M^2\,r^4 + a^2 \left(-60\,Q^4 + 108\,M\,Q^2\,r \right) \right) \cos(\theta)^2 + \\
& 2\,a^4\,r^2 \left(97\,Q^6 - 704\,M\,Q^4\,r + 1545\,M^2\,Q^2\,r^2 - 1050\,M^3\,r^3 - 222\,M\,Q^2\,r^3 + 315\,M^2\,r^4 - \right. \\
& \left. 30\,a^2 \left(Q^4 - M\,Q^2\,r \right) \right) \cos(\theta)^4 + 2\,a^6 \left(-5\,Q^6 + 100\,M\,Q^4\,r - 390\,M^2\,Q^2\,r^2 + 122\,Q^4\,r^2 + \right. \\
& \left. 420\,M^3\,r^3 - 450\,M\,Q^2\,r^3 + 315\,M^2\,r^4 + 6\,a^2 \left(Q^4 - 5\,M\,Q^2\,r \right) \right) \cos(\theta)^6 - a^8 \left(22\,Q^4 + \right. \\
& \left. 30\,M^3\,r - 240\,M\,Q^2\,r - 15\,M^2 \left(Q^2 - 27\,r^2 \right) \right) \cos(\theta)^8 + \\
& \left. \left. 15\,a^{10}\,M^2 \cos(\theta)^{10} \right) \right) \Big] \Big/ \left(a^2 + 2\,r^2 + a^2 \cos(2\,\theta) \right)^9 .
\end{aligned}
\tag{2.21}
$$

Although I_1 and I_3 are distinct, the surfaces on which they vanish have, for typical values of the hole parameters, similar shapes. Both of these invariants have 10 roots, of which two depend on the mass of the hole. The other eight roots depend only on the charge and angular momentum. The surfaces on which I_1 vanishes are shown in figures 7, 8, 9, and 10. The roots of I_3 are similar. As $a \to 0$, the roots move toward the Reissner-Nordstrøm case. The physical significance of the mass independent roots is unclear. As $a \to 0$, the two mass dependent roots move to the inner and outer horizons and the mass independent roots coalesce into the two complex roots of the Reissner-Nordstrøm case. This is shown in figure 11.

The invariant I_2 has four roots which are shown in figure 12 for a hole with $M = 2, Q = 1$, and $a = 1$. We notice that the outer root lies in the ergosphere, and that the second root weaves in and out of the inner horizon. The two remaining roots lie inside the inner horizon. In the limit $a \to 0$, the two inner roots coalesce to zero. The roots of I_2 for an extreme Kerr-Newman hole are shown in figure 13. Although it is not obvious from the figure, I_2 also vanishes on the event horizon at $\theta = 0$ and π. The two mass dependent roots remain real for some values of θ even for the ultra-extreme case where $Q^2 + a^2 > M^2$. In general none of the invariants vanishes on the horizon nor on the stationary surface, except at $\theta = 0$. Some of the roots of I_1, I_2, and I_3 are

complex for some values of a, Q and θ, as they must be, since both I_1 and I_2 have two imaginary roots for the Reissner-Nordstrøm case.

7. The γ metric

A static, axially symmetric, asymptotically flat vacuum space-time is provided by the γ metric [8], a two parameter Weyl solution. The γ metric serves as an example of a space-time where the horizon, depending on the values of the parameters M and γ, may be regular or not. The γ metric is

$$ds^2 = -\left(1 - \frac{2\,M}{r}\right)^{\gamma} dt^2 + \left(1 - \frac{2\,M}{r}\right)^{-\gamma} \left[\left(\frac{r^2 - 2Mr}{r^2 - 2Mr + M\sin\theta^2}\right)^{\gamma^2 - 1} dr^2 + \right.$$

$$\left. \frac{(r^2 - 2Mr)^{\gamma^2}}{(r^2 - 2Mr + M^2\sin\theta^2)^{\gamma^2 - 1}} d\theta^2 + (r^2 - 2Mr)\sin\theta^2 d\phi^2\right], \tag{2.22}$$

and corresponds to a total mass of γM. The γ metric reduces to the Schwarzschild metric when $\gamma = 1$. While the complete analysis of the γ metric is rather complicated, we mention only a few of the features which have a bearing on the present calculations. For $0 < \gamma < 2$, $\gamma \neq 1$ the null surface $r = 2M$ is singular along the symmetry axis $\theta = 0$ or π. For $\gamma \geq 2$ the null surface $r = 2M$ is regular along the symmetry axis. This can be seen by looking at $I_0 = R_{\alpha\beta\mu\nu}R^{\alpha\beta\mu\nu}$. We have computed both I_0 and I_1 for general θ but the results are long. Along the symmetry axis we find

$$I_0 = \frac{48\,M^2\left(1 - \frac{2\,M}{r}\right)^{2\,\gamma}\gamma^2\left(M - r + M\,\gamma\right)^2}{r^4\left(-2\,M + r\right)^4} \tag{2.23}$$

and

$$I_1 = \frac{80\,M^2\left(1 - \frac{2\,M}{r}\right)^{3\,\gamma}\gamma^2\left(3\,r^2 - 6\,M\,r\,(1 + \gamma) + 2\,M^2\,(2 + 3\,\gamma + \gamma^2)\right)^2}{r^6\left(-2\,M + r\right)^6}, \tag{2.24}$$

which reduces to the Schwarzschild result if $\gamma = 1$. I_1 vanishes on the horizon if $\gamma \geq 2$. There are also two zeros of I_1 found symmetrically about $r = M(1 + \gamma)$. In short I_1, is singular on the horizon when the horizon is singular and vanishes on the horizon when the horizon is regular. The belief that Weyl solutions are important in collapse situations hinges on the hope that reasonable interior solutions can be found for them.

B. 2+1 Black Holes

We have also computed I_1, I_2, and I_3 for the BTZ 2+1 dimensional black hole. The charged BTZ black hole found by Bañados, Teitelboim, and Zanelli [11] has a metric given by

$$ds^2 = -\left(\frac{r^2}{\sigma^2} - M + Q^2 \ln r\right) dt^2 + \left(\frac{r^2}{\sigma^2} - M + Q^2 \ln r\right)^{-1} dr^2 + r^2 d\phi^2. \tag{2.25}$$

For the charged BTZ black hole

$$I_0 = \frac{12\, r^4 + 4\, Q^2\, r^2\, \sigma^2 + 3\, Q^4\, \sigma^4}{r^4\, \sigma^4}. \tag{2.26}$$

The scalar curvature is

$$R = \frac{-(Q^2 - 6r^2/\sigma^2)}{r^2}, \tag{2.27}$$

and the invariant I_1 is

$$I_1 = \frac{20\, Q^4\, \left(-M + (r/\sigma)^2 + Q^2\, \log(r)\right)}{r^6}, \tag{2.28}$$

which is seen by inspection to vanish on the horizon. The invariant I_2 is found to be

$$I_2 = \frac{6\, Q^4\, \left(r^2 - M\, \sigma^2 + Q^2\, \sigma^2\, \log(r)\right)}{r^6\, \sigma^2}. \tag{2.29}$$

The space-time is Weyl flat, so $I_3 = 0$.

Since the geometrical and physical interpretation of the curvature invariants is unclear it may be useful to rewrite I_2 in terms of $F_{\mu\nu}$. Using the Einstein equations, we find that I_2 may be written in terms of invariants involving $F_{\mu\nu}$ and R. It is straightfoward to show that

$$I_2 = 4\left(I_{EM1} - \frac{5}{16} I_{EM2}\right) + \frac{3}{4} R_{;\lambda} R^{;\lambda}, \tag{2.30}$$

where

$$I_{EM1} = \left(F_{\mu\beta} F_\nu^\beta\right)_{;\lambda} \left(F_\beta^\mu F^{\nu\beta}\right)^{;\lambda}, \tag{2.31}$$

and

$$I_{EM2} = \left(F_{\alpha\beta} F^{\alpha\beta}\right)_{;\lambda} \left(F_{\alpha\beta} F^{\alpha\beta}\right)^{;\lambda}. \tag{2.32}$$

11

We find that

$$I_{EM1} = \frac{2\,Q^4\,\left(r^2 - M\,\sigma^2 + Q^2\,\sigma^2\,\log(r)\right)}{r^6\,\sigma^2},\tag{2.33}$$

$$I_{EM2} = \frac{4\,Q^4\,\left(r^2 - M\,\sigma^2 + Q^2\,\sigma^2\,\log(r)\right)}{r^6\,\sigma^2},\tag{2.34}$$

and

$$R_{;\lambda}R^{;\lambda} = \frac{4\,Q^4\,\left(r^2 - M\,\sigma^2 + Q^2\,\sigma^2\,\log(r)\right)}{r^6\,\sigma^2}.\tag{2.35}$$

Both the electromagnetic invariants and the scalar curvature invariant vanish on the horizon, and are in fact proportional to I_2.

The uncharged black hole space-time has constant scalar curvature and is, for our proposes, uninteresting since I_1 is identically zero.

III. CONCLUSIONS

The invariants I_1, I_2, and I_3, which are locally measurable, serve as horizon or stationary surface detectors for a variety of space-times but not for Kerr-Newman black holes. We have shown that I_1 serves as a horizon detector for any Schwarzschild like space-time and conjecture that I_1 serves as a horizon detector for regular horizons in any static axially symmetric space-time.

It is not known if an invariant can be found that will vanish on the horizon in the Kerr-Newman case.

A problem of considerable current interest in numerical general relativity is the detection of emerging horizons in collapse problems. The invariants discussed here, particularly I_1 and I_2, may be useful tools for the numerical detection of such emerging horizons.

IV. ACKNOWLEDGMENTS

REFERENCES

[1] E. Seidel and W.-M. Suen, Phys. Rev. Lett. **69**, p.1845, 1992.

[2] Thomas W. Baumgarte, Gregory B. Cook, Mark A. Scheel, Stuart L. Shapiro and Saul A. Teukolsky, Phys. Rev. D. **54** p. 4849 ,1996.

[3] Jonathan Thornburg, Phys. Rev. D. **54**, p. 4899, 1996.

[4] Anders Karlhede, Ulf Lindström and Jan Åman, Gen. Rel. Grav. **14** p. 569, 1982.

[5] Charles W. Misner, Kip S. Thorne and John Archibald Wheeler, *Graviatation*, W. H. Freeman, San Francisco, 1973.

[6] Riso Tammelo and Üllar Kask, Gen. Rel. Grav. **29** p. 997, 1997.

[7] Anders Karlhede, Gen. Rel. Grav. **12** p. 693, 1979.

[8] F. Paul Esposito and Louis Witten, Phys.Lett. **58B**, p. 357, 1975.

[9] See for example Robert M. Wald *General Relativity*, p. 320, University of Chicago Press, Chicago, 1984

[10] See for example S.W. Hawking and G. F. R. Ellis *The large scale structure of space-time*, p 163, Cambridge University Press, Cambridge, 1973.

[11] M. Bañados, C. Teitelboim and J. Zanelli, Phys. Rev. Lett. **69**, p. 1849 1992.

$$r = \left(1 + \sqrt{2} + \sqrt{4 + 2\sqrt{2}}\right) a \cos(\theta)$$

$$r = -\left(\left(1 + \sqrt{2} + \sqrt{4 + 2\sqrt{2}}\right) a \cos(\theta)\right)$$

$$r = \left(1 + \sqrt{2} - \sqrt{4 + 2\sqrt{2}}\right) a \cos(\theta)$$

$$r = \left(-1 - \sqrt{2} + \sqrt{4 + 2\sqrt{2}}\right) a \cos(\theta)$$

$$r = \left(-1 + \sqrt{2}\right) a \cos(\theta) + \sqrt{4 - 2\sqrt{2}}\sqrt{a^2 \cos(\theta)^2}$$

$$r = -\left(\left(-1 + \sqrt{2}\right) a \cos(\theta)\right) - \sqrt{4 - 2\sqrt{2}}\sqrt{a^2 \cos(\theta)^2}$$

$$r = -\left(\left(-1 + \sqrt{2}\right) a \cos(\theta)\right) + \sqrt{4 - 2\sqrt{2}}\sqrt{a^2 \cos(\theta)^2}$$

$$r = \left(-1 + \sqrt{2}\right) a \cos(\theta) - \sqrt{4 - 2\sqrt{2}}\sqrt{a^2 \cos(\theta)^2}$$

TABLE I. The eight roots of $I_1 = 0$ that are independent of the mass of the hole for the Kerr solution.
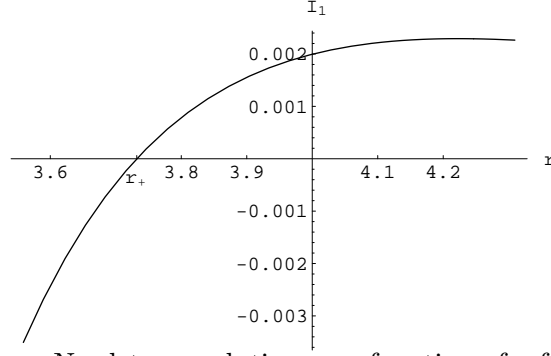
FIG. 1. I_1 for the Reissner-Nordstrøm solution as a function of r for the case $M = 2, Q = 1$ in the vicinity of r_+
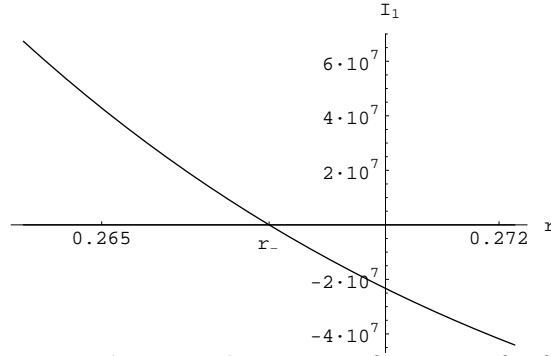
FIG. 2. I_1 for the Reissner-Nordstrøm solution as a function of r for the case $M = 2, Q = 1$ in the vicinity of r_-
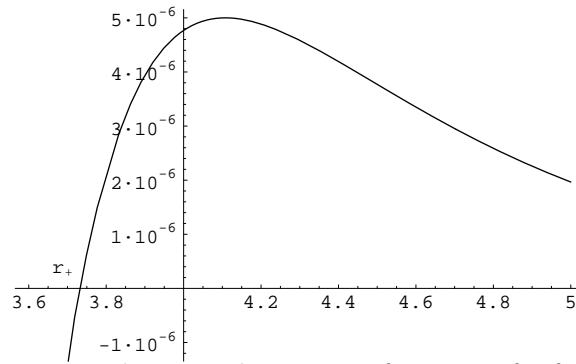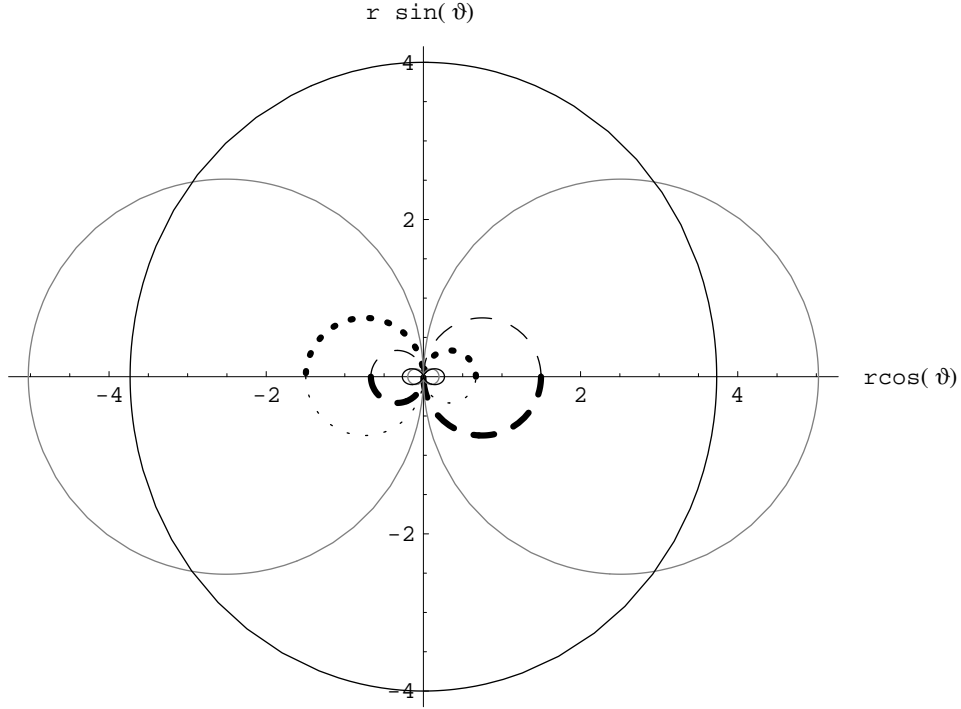
FIG. 3. I_2 for the Reissner-Nordstrøm solution as a function of r for the case $M = 2, Q = 1$ in the vicinity of r_+
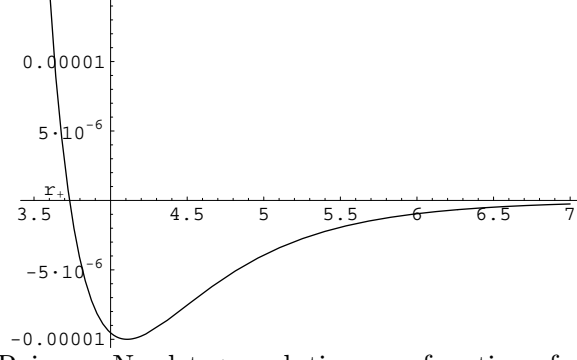
FIG. 4. $I_3 - I_1$ for the Reissner-Nordstrøm solution as a function of r for the case $M = 2, Q = 1$ in the vicinity of r_+

FIG. 5.   The roots of I_1 for the Kerr metric. The inner and outer stationary surfaces are shown in black. There is a root on each stationary surface. Four other roots are shown in grey. The remaining four roots are shown as dashed lines with a different dashing used for each root. Two of the roots are inside the inner stationary surface and are thus hard to see. All the roots except the two which lie on the stationary surfaces depend only on a.

17
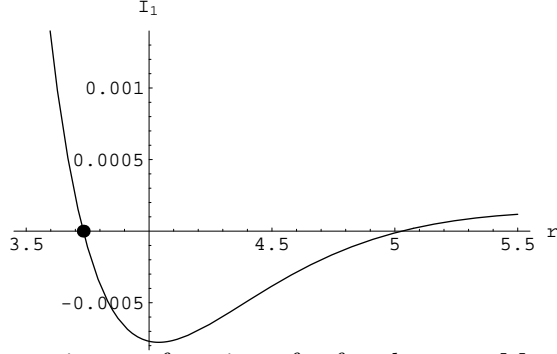
FIG. 6. I_1 or the Kerr metric as a function of r for the case $M = 2, a = 1$. The approach is along the $\theta = 0$ axis and the stationary limit is indicated by the black dot.
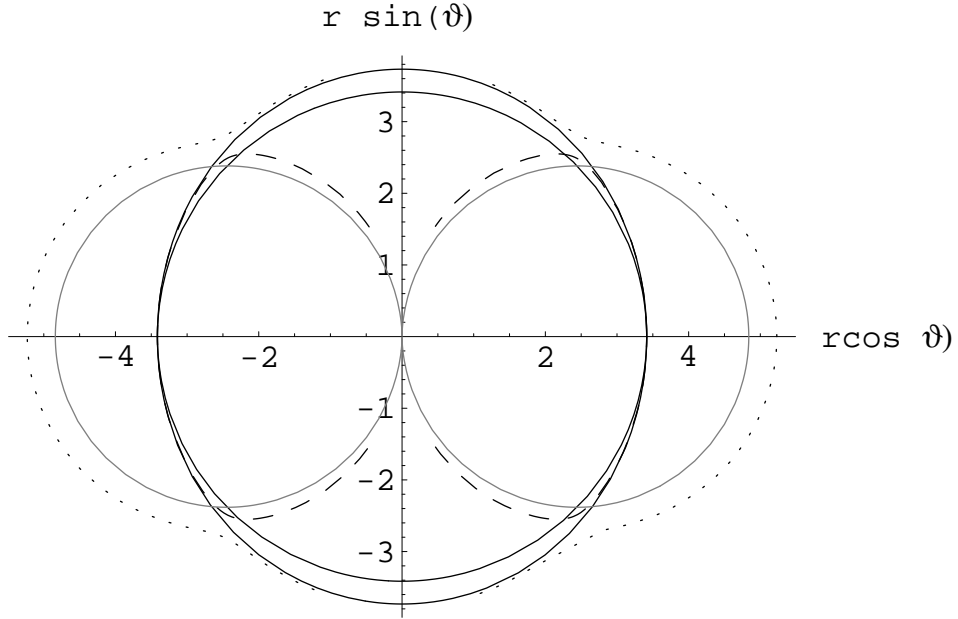
FIG. 7. The outer roots of I_1 for the Kerr-Newman metric with $M = 2, a = 1, Q = 1$. The horizon and outer stationary surfaces are shown in black. The three outer roots are shown in gray and as dashed lines.
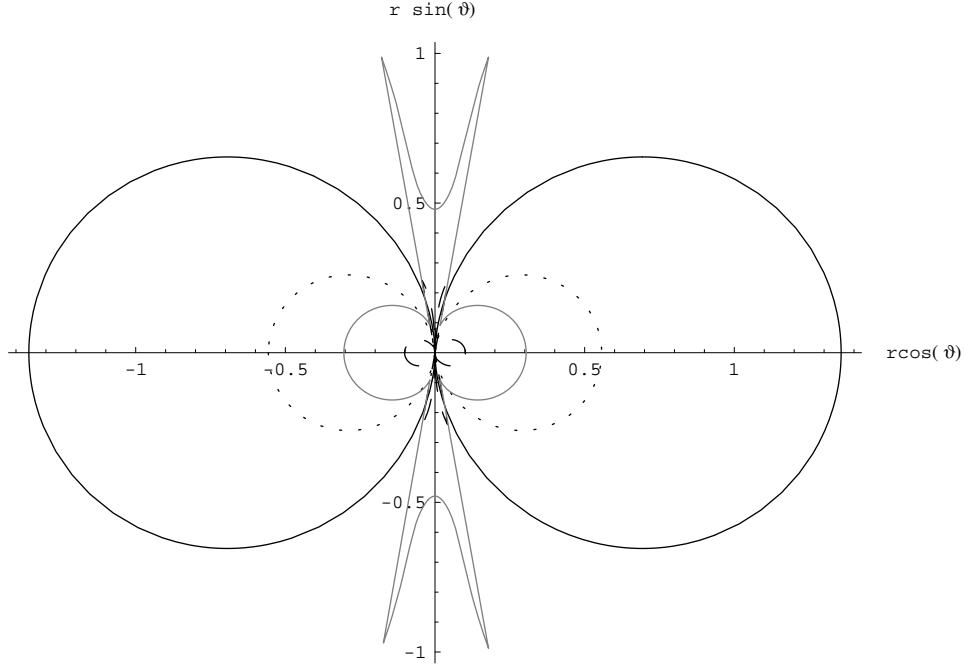
FIG. 8.   Four of the inner roots of I_1 for the Kerr-Newman metric with $M = 2, a = 1, Q = 1$.

A close up view of the inner most root is shown in figure 9.
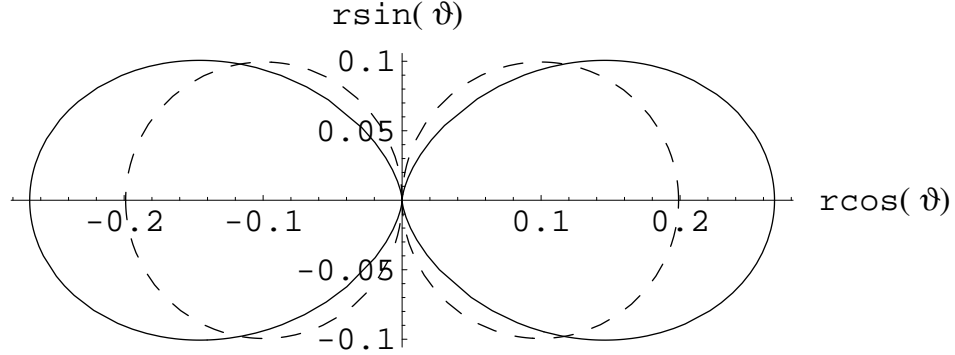

FIG. 9.   The inner most root (shown with a dashed line) of I_1 and the inner stationary surface

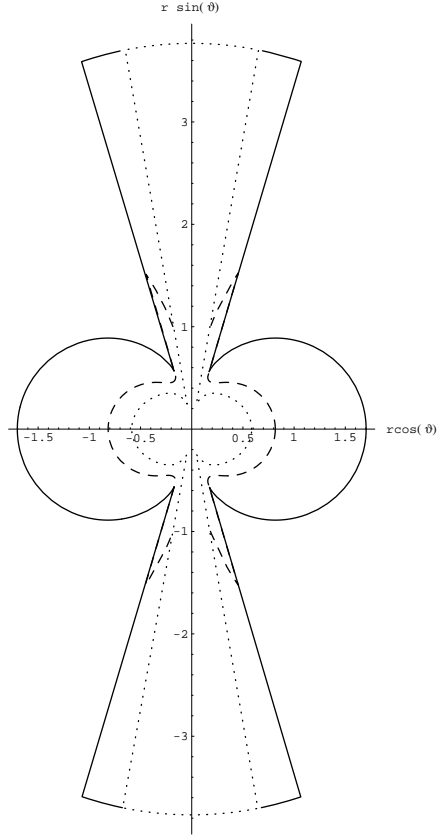(shown in black) for the Kerr-Newman metric with $M = 2, a = 1, Q = 1$.

FIG. 10. The other three inner roots of I_1 for the Kerr-Newman metric with $M = 2, a = 1, Q = 1$. These roots all lie outside the inner stationary surface.
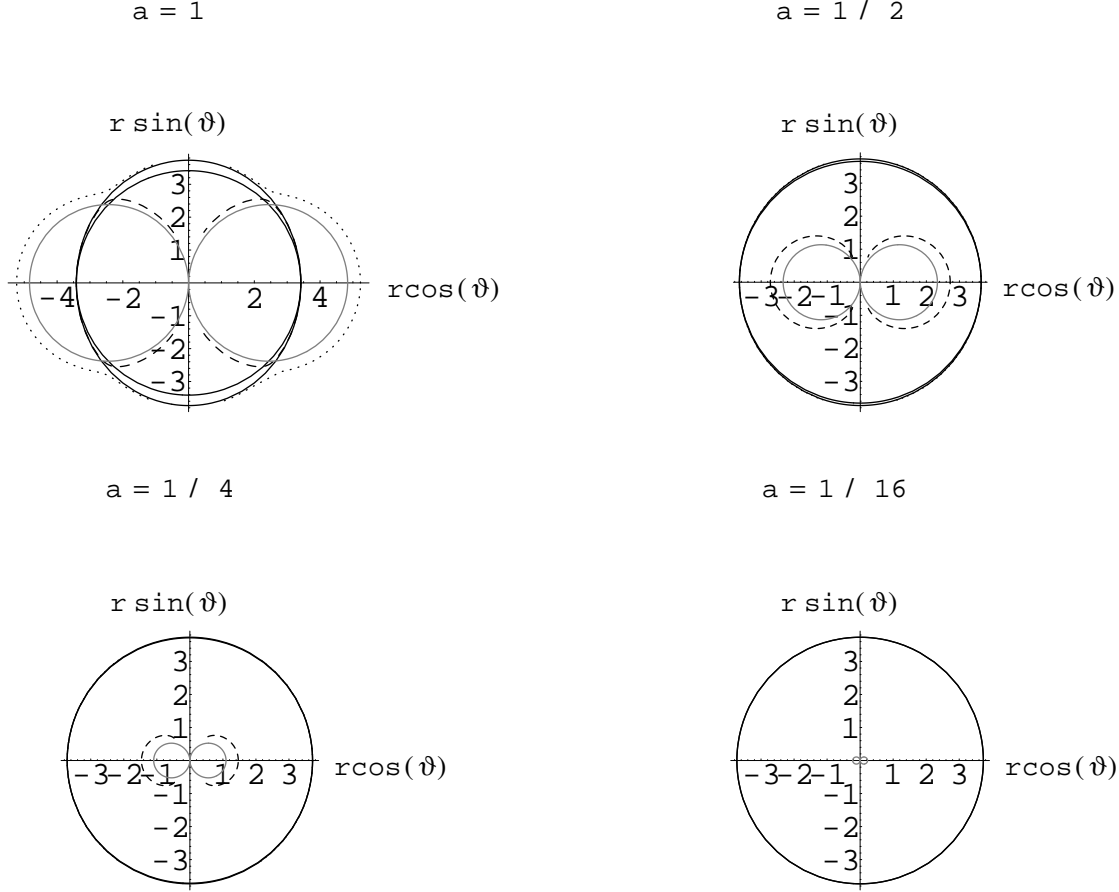
a = 1

r sin(ϑ)

rcos(ϑ)

a = 1 / 2

r sin(ϑ)

rcos(ϑ)

a = 1 / 4

r sin(ϑ)

rcos(ϑ)

a = 1 / 16

r sin(ϑ)

rcos(ϑ)

FIG. 11. The three outer roots of I_1 for the Kerr-Newman metric as $a \to 0$ with $M = 2, Q = 1$. As the hole spins down the roots move toward the Reissner-Nordstrøm case. The outer horizon and stationary surface are shown in black. The two mass dependent roots move to the inner and outer horizons and the mass independent roots coalesce into the two complex roots of the Reissner-Nordstrøm case. For reasons of scale only one of the mass independent roots is shown. The root shown with the dashed line becomes complex as $a \to 0$.
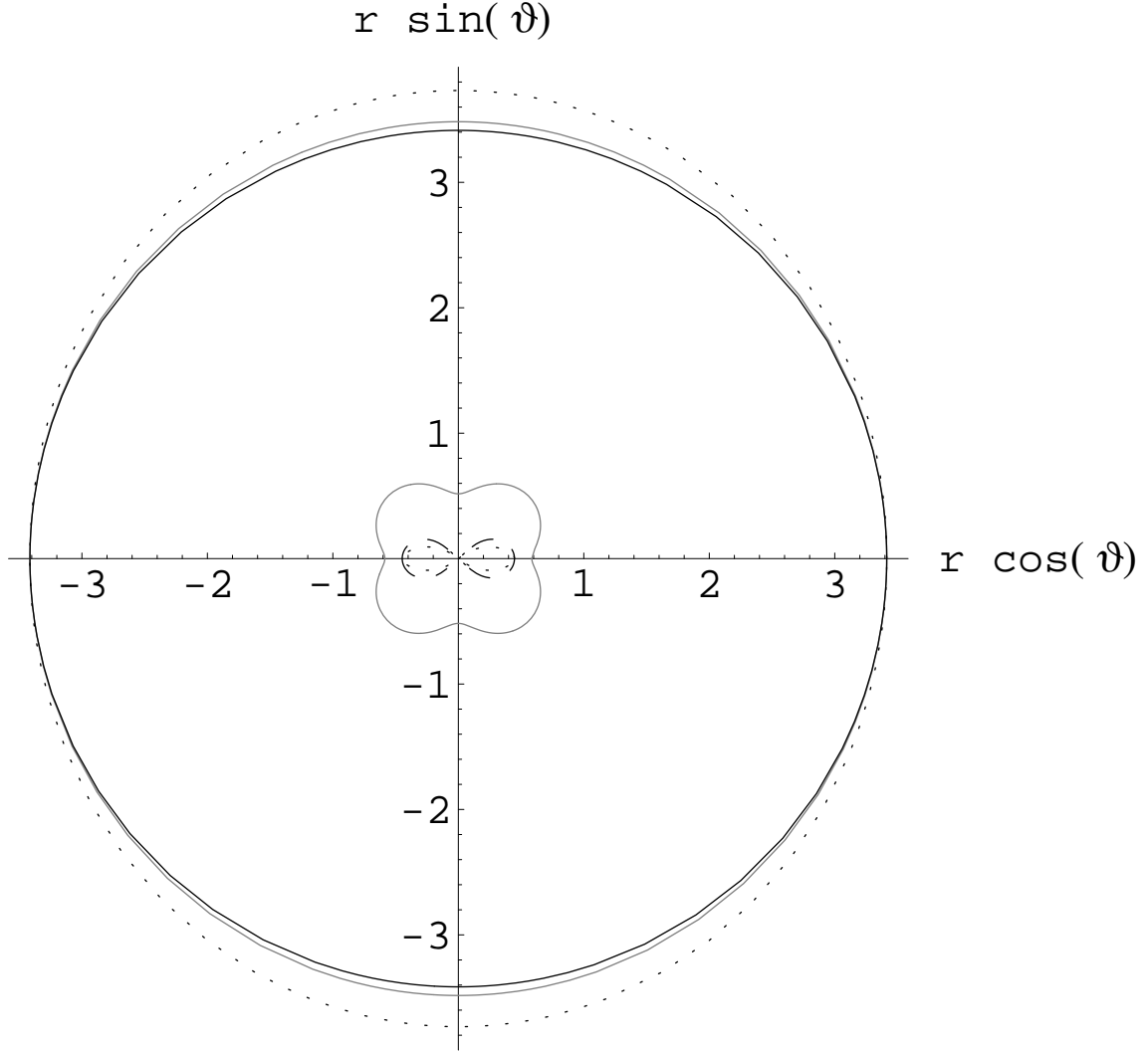
FIG. 12. The four roots of I_2 for the Kerr-Newman metric for $M = 2, a = 1, Q = 1$. The outer root, shown in gray, is trapped in the ergosphere. The stationary limit is show as a dashed line, the event horizon is shown in black. The inner gray root weaves in and out of the inner horizon which is not shown.
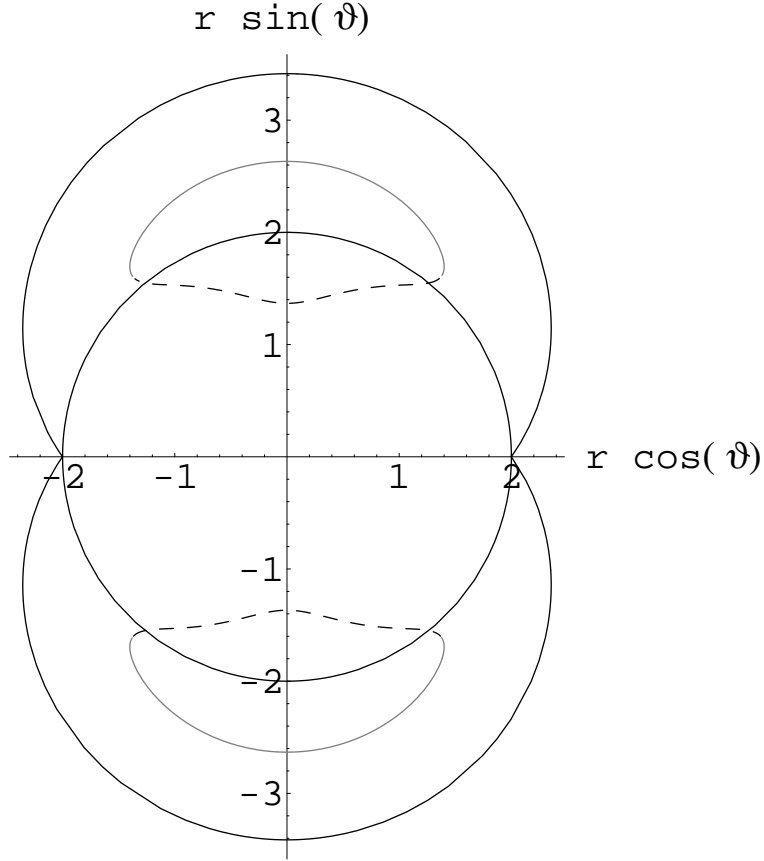
FIG. 13. The two outer roots of I_2 for the Kerr-Newman metric for an extreme case with $M = 2, a = 2^{1/2}, Q = 2^{1/2}$. The two outer roots have joined each other. The light gray line shows the same root as the outer gray line in figure 12. The dashed line is same root as the inner gray root in figure 12. The horizon and the stationary surface are shown in black.